



**HAL**  
open science

## Interneuronal correlations dynamically adjust to task demands at multiple time-scales

S Ben Hadj Hassen, C Gaillard, E Astrand, C Wardak, S. Ben Hamed

► **To cite this version:**

S Ben Hadj Hassen, C Gaillard, E Astrand, C Wardak, S. Ben Hamed. Interneuronal correlations dynamically adjust to task demands at multiple time-scales. 2020. hal-03045220

**HAL Id: hal-03045220**

**<https://hal.science/hal-03045220>**

Preprint submitted on 7 Dec 2020

**HAL** is a multi-disciplinary open access archive for the deposit and dissemination of scientific research documents, whether they are published or not. The documents may come from teaching and research institutions in France or abroad, or from public or private research centers.

L'archive ouverte pluridisciplinaire **HAL**, est destinée au dépôt et à la diffusion de documents scientifiques de niveau recherche, publiés ou non, émanant des établissements d'enseignement et de recherche français ou étrangers, des laboratoires publics ou privés.



## 17 **Summary**

18 Functional neuronal correlations between pairs of neurons are thought to play an important  
19 role in neuronal information processing and optimal neuronal computations during attention,  
20 perception, decision-making and learning. Here, we report dynamic changes in prefrontal  
21 neuronal noise correlations at multiple time-scales, as a function of task contingencies.  
22 Specifically, we record neuronal activity from the macaque frontal eye fields, a cortical region  
23 at the source of spatial attention top-down control, while the animals are engaged in tasks of  
24 varying cognitive demands. We show that the higher the task demand and cognitive  
25 engagement the lower noise correlations. We further report that within a given task, noise  
26 correlations significantly decrease in epoch of higher response probability. Last we show that  
27 the power of the rhythmic modulations of noise correlations in the alpha and beta frequency  
28 ranges also decreases in the most demanding tasks. All of these changes in noise correlations  
29 are associated with layer specific modulations in spikes-LFP phase coupling, suggesting both  
30 a long-range and a local intra-areal origin. Over all, this indicates a highly dynamic  
31 adjustment of noise correlations to ongoing task requirements and suggests a strong functional  
32 role of noise correlations in cognitive flexibility.

33

## 34 ***Significance statement***

35 Cortical neurons are densely interconnected. As a result, pairs of neurons share some degree  
36 of variability in their neuronal responses. This impacts how much information is present  
37 within a neuronal population and is critical to attention, decision-making and learning. Here  
38 we show that, in the prefrontal cortex, this shared inter-neuronal variability is highly flexible,  
39 decreasing across tasks as cognitive demands increase and within trials in epochs of maximal  
40 behavioral demand. It also fluctuates in time at a specific rhythm, the power of which  
41 decreases for higher cognitive demand. All of these changes in noise correlations are  
42 associated with layer specific modulations in spikes-LFP phase coupling. Over all, this  
43 suggests a strong functional role of noise correlations in cognitive flexibility.

44

45

## 46 **Introduction**

47           Optimal behavior is the result of interactions between neurons both within and across  
48 brain areas. Identifying how these neuronal interactions flexibly adjust to the ongoing  
49 behavioral demand is key to understand the neuronal processes and computations underlying  
50 optimal behavior. Several studies have demonstrated that functional neuronal correlations  
51 between pairs of neurons, otherwise known as noise correlations, play an important role in  
52 perception and decision-making<sup>1-9</sup>. Specifically, several experimental and theoretical studies  
53 show that noise correlations have an impact on the amount of information that can be decoded  
54 for neuronal populations<sup>4,10-12</sup> as well as on overt behavioral performance<sup>4,10-15</sup>. As a result,  
55 understanding how noise correlations dynamically adjust to task demands is a key step toward  
56 clarifying how neural circuits dynamically control information transfer, thereby optimizing  
57 behavioral performance.

58           Several sources of noise correlations have been proposed, ranging from shared  
59 connectivity<sup>16</sup>, to global fluctuations in the excitability of cortical circuits<sup>17,18</sup>, feedback  
60 signals<sup>19</sup> or internal areal dynamics<sup>20-22</sup>, or bottom-up peripheral sensory processing<sup>23</sup>. In an  
61 independent study<sup>24</sup>, we for example show that noise correlations in the prefrontal cortex  
62 fluctuate rhythmically in the high alpha (10-16Hz) and beta (20-30Hz) frequency ranges. We  
63 further show that these rhythmic fluctuations co-occur with changes in spike-LFP phase  
64 coupling and can be segregated into a long-range component, possibly reflecting global  
65 fluctuations in the excitability of the functional network of interest, as well as to local internal  
66 areal dynamics. Importantly, these fluctuations account for variability in behavioral  
67 performance.

68           From a cognitive point of view, noise correlations have been shown to change as a function of  
69 spatial attention<sup>25</sup>, spatial memory<sup>26</sup> and learning<sup>27,28</sup>, suggesting that they are subject both to  
70 rapid dynamic changes as well as to longer term changes, supporting optimal neuronal  
71 computations<sup>28</sup>.

72           Here, we focus onto how the strength of rhythmic modulation of noise correlations, in  
73 the prefrontal cortex, is affected by the ongoing task at multiple time-scales. Specifically, we  
74 record neuronal activity from the macaque frontal eye fields, a cortical region which has been  
75 shown to be at the source of spatial attention top-down control<sup>15,29-31</sup> while the animals are  
76 engaged in tasks of varying cognitive demands, as assessed by their overt behavioral  
77 performance. Overall, we show that noise correlations vary in strength both as a function of  
78 the ongoing task as well as a function of the probabilistic structure of the task, thus adjusting

79 dynamically to ongoing behavioral demands. Importantly, we show that these variations of  
80 noise correlations strength across tasks co-occur with cortical layer specific variations in  
81 spikes-LFP phase coupling.

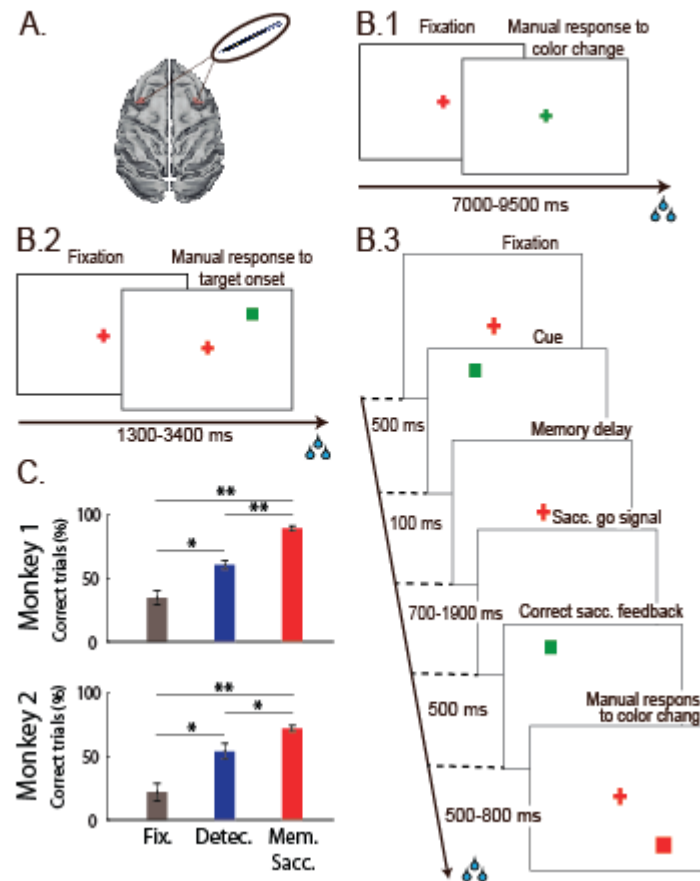
## 82 **Results**

83 Our main goal in this work is to examine how the degree of cognitive engagement and  
84 task demands impact the neuronal population state as assessed from inter-neuronal noise  
85 correlations. Cognitive engagement was operationalized through tasks of increasing  
86 behavioral requirements. The easiest task (*Fixation task*, figure 1B.1) is a central fixation task  
87 in which monkeys are required to detect an unpredictable change in the color of the fixation  
88 point, by producing a manual response within 150 to 800ms from color change. The second  
89 task (*Target detection task*, figure 1B.2) adds a spatial uncertainty on top of the temporal  
90 uncertainty of the event associated with the monkeys' response. It is a target detection task, in  
91 which the target can appear at one of four possible locations, at an unpredictable time from  
92 fixation onset. The monkeys have to respond to this target presentation by producing a manual  
93 response within 150 to 800ms from color change. In the third task (*Memory guided saccade*  
94 *task*, figure 1B.3), monkeys are required to hold the position of a spatial cue in memory for  
95 700 to 1900ms and to perform a saccade towards that memorized spatial location on the  
96 presentation of a go signal. This latter task thus involves a temporal uncertainty but no spatial  
97 uncertainty. However, in contrast with the previous tasks, it requires the production of a  
98 spatially oriented oculomotor response rather than a simple manual response. Accordingly,  
99 both monkeys have higher performances on the memory guided saccade task than on the  
100 target detection task (Figure 1C, Wilcoxon rank sum test, Monkey 1,  $p < 0.01$ , Monkey 2,  
101  $p < 0.05$ ), and higher performances on the target detection task than on the fixation task  
102 (Wilcoxon rank sum test,  $p < 0.05$ ). Importantly, task order was randomized from one session  
103 to the next, such that the reported effects could not be accounted for by fatigue or satiation  
104 effects.

105 Neuronal recordings were performed in the prefrontal cortex, specifically in the frontal  
106 eye field (FEF, figure 1A), a structure known to play a key role in covert spatial attention<sup>31-34</sup>.  
107 In each session, multi-unit activity (MUA) and local field potential (LFP) were recorded  
108 bilaterally, while monkeys performed these three tasks. In the following, noise correlations  
109 between the different prefrontal signals of the same hemisphere were computed on equivalent  
110 task fixation epochs, away from both sensory intervening events and motor responses. We

111 analyzed how these noise correlations varied both across tasks, as a function of cognitive  
 112 engagement and within-tasks, as a function of the probabilistic structure of the task.

113



114

115 **Figure 1:** (A) *Recordings sites.* On each session, 24-contacts recording probes were placed in  
 116 the left and right FEFs. (B.1) *Fixation task.* Monkeys had to fixate a red central cross and  
 117 were rewarded for producing a manual response 150ms to 800ms following fixation cross  
 118 color change. (B.2) *Target detection task.* Monkeys had to fixate a red central cross and were  
 119 rewarded for producing a manual response 150ms to 800ms from the onset of a low  
 120 luminosity target at an unpredictable location out of four possible locations on the screen.  
 121 (B.3) *Memory-guided saccade task.* Monkeys had to fixate a red central cross. A visual cue  
 122 was briefly flashed in one of four possible locations on the screen. Monkeys were required to  
 123 hold fixation until the fixation cross disappeared and then produce a saccade to the spatial  
 124 location indicated by the cue within 300ms from fixation point offset. On success, the cue re-  
 125 appeared and the monkeys had to fixate it. They were then rewarded for producing a manual  
 126 response 150ms to 800ms following the color change of this new fixation stimulus. (C)  
 127 *Behavioral performance.* Average percentage of correct trials across sessions for each task  
 128 and each monkey with associated standard errors.

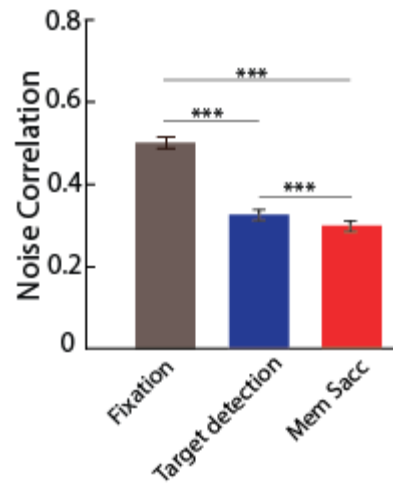
129

130            *Noise correlations decrease as cognitive engagement and task requirements*  
131 *increase.*

132            In order to characterize how inter-neuronal noise correlations vary as a function of  
133 cognitive engagement and task requirements, we proceeded as follows. In each session  
134 (n=26), noise correlations were computed between each pair of task-responsive channels  
135 (n=671, see Methods), over equivalent fixation task epochs, running from 300 to 500 ms after  
136 eye fixation onset. This epoch was at a distance from a possible visual or saccadic foveation  
137 response and in all three tasks, monkeys were requested to maintain fixation at this stage. It  
138 was also still early on in the trial, such that no intervening sensory event was to be expected  
139 by the monkey at this time. Importantly, fixation behavior, i.e. the distribution of eye position  
140 in within the fixation window, did not vary between the different tasks (Friedman test,  
141  $p < 0.001$ ). As a result, and because tasks were presented in blocks, any difference in noise  
142 correlations across tasks during this “neutral” fixation epoch are to be attributed to general  
143 non-specific task effects, i.e. differences in the degree of cognitive engagement and task  
144 demands. Noise correlations were significantly different between tasks (figure 2, ANOVA,  
145  $p < 0.001$ ). Specifically, they were higher in the fixation task than in the target detection task  
146 (figure 2, Wilcoxon rank sum test,  $p < 0.001$ ) and in the memory guided saccade task  
147 (Wilcoxon rank sum test,  $p < 0.001$ ). They were also significantly higher in the target detection  
148 task than in the memory guided saccade task (Wilcoxon rank sum test,  $p < 0.001$ ). Importantly,  
149 these significant changes in noise correlations existed in the absence of significant differences  
150 in mean firing rate (ANOVA,  $p > 0.5$ ), standard error around this mean firing rate (ANOVA,  
151  $p > 0.6$ ), and Fano factor (ANOVA,  $p > 0.7$ ). These task differences in noise correlations were  
152 preserved as noise correlations decreased as a function on the cortical distance between the  
153 neuronal pairs (figure S1A). These task differences were also preserved across pairs sharing  
154 the spatial functional selectivity or not (figure S1B). We thus describe that, in absence of any  
155 sensory or cognitive processing, noise correlations are strongly modulated by cognitive  
156 engagement and task demands.

157

158



159

160

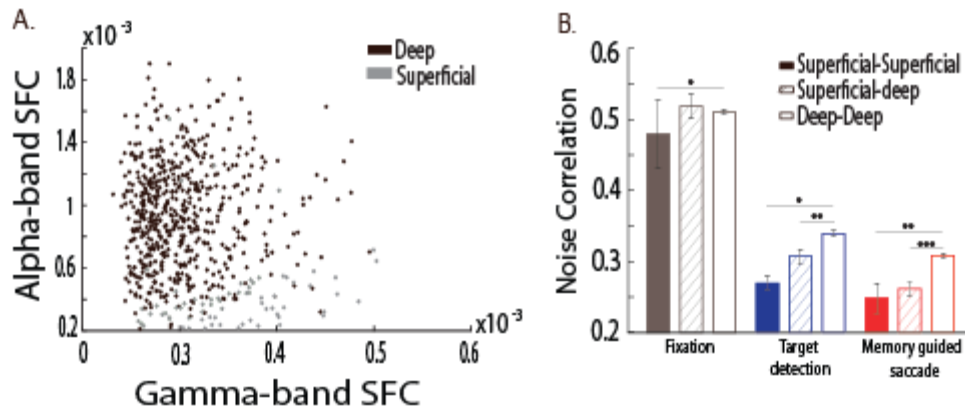
161 **Figure 2: Noise correlations as a function of task.** Average noise correlations across  
162 sessions for each of the three tasks (mean +/- s.e., noise correlations calculated on the  
163 neuronal activities from 300 to 500 after eye fixation onset. Grey: fixation task; blue: target  
164 detection task; red: memory guided saccade task. Stars indicate statistical significance  
165 following a one-way ANOVA; \* $p < 0.05$ ; \*\* $p < 0.01$ ; \*\*\* $p < 0.001$ .

166 The task differences in noise correlations described above could reflect changes in the  
167 shared functional connectivity, within the large-scale parieto-frontal functional network the  
168 cortical region of interest belongs to<sup>16</sup> or to global fluctuations in the excitability of cortical  
169 circuits<sup>35,36</sup>. This large-scale hypothesis predicts that the observed changes in noise  
170 correlations are independent from intrinsic connectivity as assessed by the distance, the spatial  
171 selectivity and the cortical layer between the pairs of signals across which noise correlations  
172 are computed. Alternatively, these task differences in noise correlations could reflect a more  
173 complex reweighing of functional connectivity and the excitatory/inhibitory balance in the  
174 area of interest, due to local changes in the random shared fluctuations in the pre-synaptic  
175 activity of cortical neurons<sup>4,16,37,38</sup>. This local hypothesis predicts that the observed changes  
176 in noise correlations depend onto intrinsic microscale connectivity.

177 FEF neurons are characterized by a strong visual, saccadic, spatial memory and spatial  
178 attention selectivity<sup>31,39,40</sup>. Previous studies have shown that pure visual neurons are located  
179 in the input layers of the FEF while visuo-motor neurons are located in its output layers<sup>39,41–</sup>  
180<sup>45</sup>. Independently, it has been shown that, in extrastriate area V4, the ratio between the alpha  
181 and gamma spike field coherence discriminated between LFP signals in deep (low alpha /

182 gamma spike field coherence ratio) or superficial cortical layers (high alpha / gamma spike  
183 field coherence ratio)<sup>46</sup>. In our own data, because our recordings were performed tangentially  
184 to FEF cortical surface, we have no direct way of assigning the recorded MUAs to either  
185 superficial or deep cortical layers. However, the alpha / gamma spike field coherence ratio  
186 provides a very reliable segregation of visual and visuo-motor MUAs (figure 3A). We thus  
187 consider that, as has been described for area V4, this measure allows for a robust delineation  
188 of superficial and deep layers in area FEF. In the following, we computed inter-neuronal noise  
189 correlations between three different categories of pairs based on their assigned cortical layer:  
190 superficial/superficial pairs, superficial/deep pairs and deep/deep pairs, where superficial  
191 MUA correspond to predominantly visual, low alpha/gamma spike field coherence ratio  
192 signals and deep MUA correspond to predominantly visuo-motor, high alpha/gamma spike  
193 field coherence ratio signals. Noise correlations varied as a function of cortical layer (Figure  
194 3B). This cortical layer effect was present for all tasks and expressed independently of the  
195 main task effect described above (2-way ANOVA, Task x Cortical layer, Task effect:  
196  $p < 0.001$ ; Cortical layer effect:  $p < 0.001$ ). Layer effects were not constant across tasks,  
197 possibly suggesting task-dependent functional changes in within and across layer neuronal  
198 interactions (interaction:  $p < 0.05$ ). Unexpectedly, belonging to the same layer cortical layer  
199 didn't systematically maximize noise correlations. Indeed, post-hoc analyses indicate  
200 significantly lower noise correlations between the superficial/superficial pairs as compared to  
201 the deep/deep pairs (Wilcoxon rank sum test, Fixation task:  $p < 0.05$ ; Target detection task:  
202  $p < 0.05$ ; Memory-guided saccade task:  $p < 0.01$ ). Superficial/deep pairs sat in between these  
203 two categories and had significantly lower noise correlations than the deep/deep pairs  
204 (Wilcoxon rank sum test, Fixation task:  $p < 0.05$ ; Target detection task:  $p < 0.05$ ; Memory-  
205 guided saccade task:  $p < 0.01$ ) and higher noise correlations than the superficial/superficial  
206 pairs, though this difference was never significant.

207



208

209 **Figure3:** (A) Distribution of alpha spike-LFP coupling (6-16Hz) as a function of gamma (40-  
210 60Hz) spike-LFP coupling for visual and visuomotor frontal eye field sites. Sites with visual  
211 selectivity but no motor selectivity (grey, putative superficial sites) demonstrated stronger  
212 gamma-band spike-LFP phase coupling, whereas sites with visuomotor selectivity (black,  
213 putative deep sites) demonstrated stronger alpha-band spike-LFP coupling. (B) Noise  
214 correlations as a function of pair functional selectivity. Average of noise correlations (mean  
215  $\pm$  s.e.) across sessions, for each task, from 300ms to 500ms after eye fixation onset, as a  
216 function of pair functional selectivity: visual-visual, visual-visuomotor, visuomotor-  
217 visuomotor. Stars indicate statistical significance following a two-way ANOVA and ranksum  
218 post-hoc tests; \*p<0.05; \*\*p<0.01; \*\*\*p<0.001.

219 Overall, these observations support the co-existence of both a global large-scale  
220 change as well as a local change in functional connectivity. Indeed, task effects onto noise  
221 correlations build up onto cortical distance, spatial selectivity and cortical layer effects,  
222 indicating global fluctuations in the excitability of cortical circuits<sup>35,36</sup>. On top of this global  
223 effect, we also note more complex changes as reflected from statistical interactions between  
224 task and spatial selectivity or layer attribution effects. This points towards more local changes  
225 in neuronal interactions, based on both 1) functional neuronal properties such as spatial  
226 selectivity that may change across tasks<sup>47-50</sup> and 2) the functional reweighing of top-down  
227 and bottom-up processes<sup>29,31</sup>.

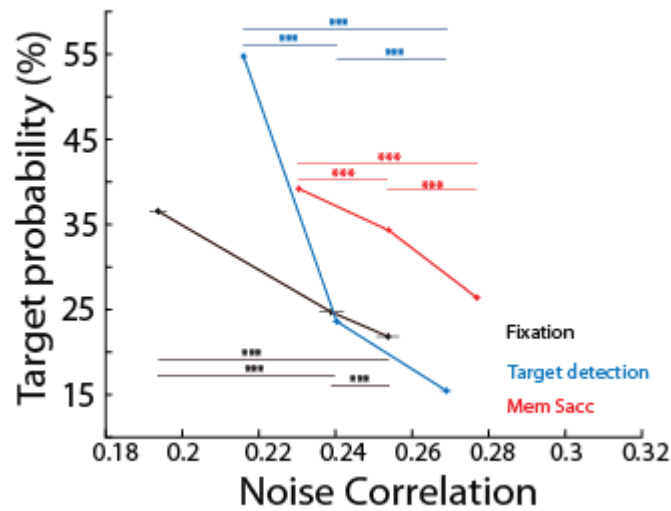
### 228 ***Impact of the probabilistic structure of the task onto noise correlations.***

229 The variation of noise correlations as a function of cognitive engagement and task  
230 demands suggests a flexible adaptive mechanism that adjusts noise correlations to the ongoing  
231 behavior. On task shifts, this mechanism probably builds up during the early trials of the new  
232 task, past trial history affecting noise correlations in the current trials. In a previous study<sup>51</sup>,  
233 we show that, in a cued target detection task, while noise correlations are higher on miss trials

234 than on hit trials, noise correlations are also higher on both hit and miss trials, when the  
235 previous trial was a miss as compared to when it was a hit. Here, one would expect that on the  
236 first trials of task shifts, noise correlations would be at an intermediate level between the  
237 previous and the ongoing task. Task shifts being extremely rare events in our experimental  
238 protocol, this cannot be confirmed. On top of this slow dynamics carry on effect, one can also  
239 expect faster dynamic adjustments to the probabilistic structure of the task. This is what we  
240 demonstrate below.

241 In each of the three tasks, target probability (saccade go signal probability in the case  
242 of the memory guided saccade task) varied as a function of time. As a result, early target onset  
243 trials had a different target probability compared to intermediate and late target onset trials.  
244 Our prediction was that if monkeys had integrated the probabilistic structure of the task, this  
245 should reflect onto a dynamic adjustment of noise correlations as a function of target  
246 probability. Figure 4 confirms this prediction. Specifically, for all tasks, noise correlations  
247 were lowest in task epochs with highest target probability (Wilcoxon non-parametric test,  
248  $p < 0.001$  for all pair-wise comparisons). These variations between the highest and lowest  
249 target probability epochs were highly significant and in the order of 15% or more (Fixation  
250 task: 15%, Target detection task: 40%, Memory-guided saccade task: 14%). This variation  
251 range was lower than the general task effect we describe above but yet quite similar across  
252 tasks. Overall, this indicates that noise correlations in addition to being dynamically adjusted  
253 to task structure, are also dynamically adjusted to trial structure, and are lowest at the time of  
254 highest behavioral demand in the trial.

255



256

257 **Figure4: Noise correlations decrease as function of expected response probability.** Average  
258 noise correlations (mean +/- s.e.) across sessions, for each task, calculated on 200ms before  
259 the target (fixation and target detection tasks) onset or saccade execution signal onset  
260 (memory guided saccade task), as a function of expected target probability. Each data point  
261 corresponds to noise correlations computed over trials of different fixation onset to event  
262 response intervals, i.e. over trials of different expected response probability. Stars indicate  
263 statistical significance following a two-way ANOVA and ranksum post-hoc tests; \* $p < 0.05$ ;  
264 \*\* $p < 0.01$ ; \*\*\* $p < 0.001$ .

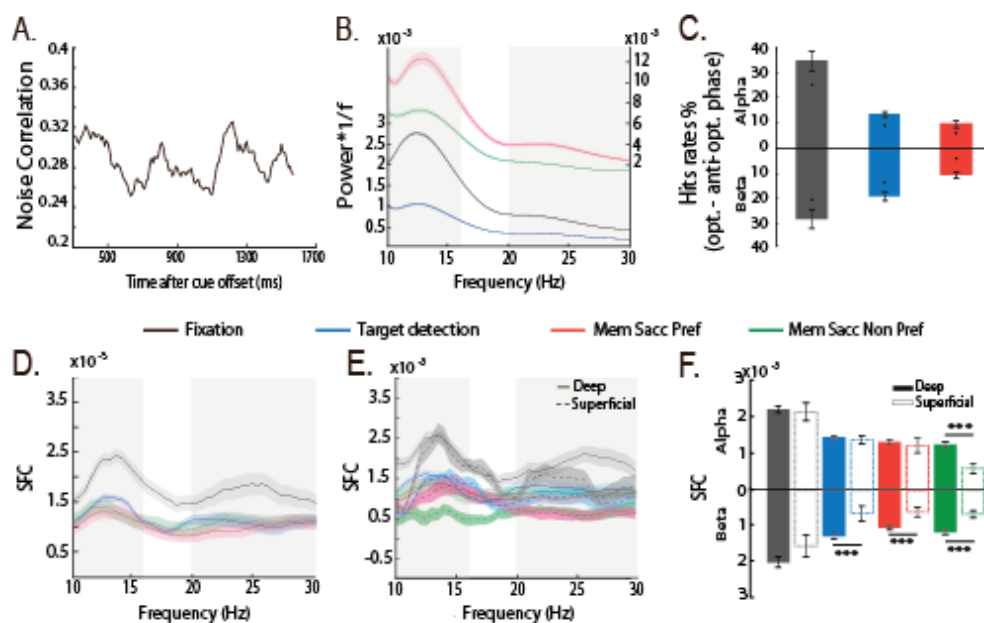
#### 265 *Strength of rhythmic fluctuations in noise correlations as a function of tasks*

266 In an independent study <sup>24</sup>, we show that noise correlations in the prefrontal cortex  
267 fluctuate rhythmically in the high alpha (10-16Hz) and beta (20-30Hz) frequency ranges. This  
268 is reproduced here in three distinct tasks (figure 5A). Noise correlations phase locked to  
269 fixation onset (Fixation and target detection task) or cue presentation (Memory guided  
270 saccade task) are characterized by rhythmic fluctuations in two distinct frequency ranges: a  
271 high alpha frequency range (10-16 Hz) and a beta frequency range (20-30Hz), as quantified  
272 by a wavelet analysis (figure 5B). These oscillations can be described in all of the three tasks,  
273 this in spite of an overall higher background spectral power during the memory guided  
274 saccade task, both when noise correlations are calculated on trials in which spatial memory  
275 was instructed towards the preferred or the non-preferred location of the MUA signals (figure  
276 5B, red and green curves respectively). Because spatial selective processes are at play in the  
277 memory guided saccade task, both for trials in which spatial memory is oriented towards the  
278 preferred MUA location (excitatory processes) or towards the non-preferred location  
279 (inhibitory processes), we will mostly focus on the fixation and the target detection tasks.

280 When compensating the rhythmic modulations of noise correlations for background power  
 281 levels (assuming an equal frequency power between all conditions beyond 30Hz), frequency  
 282 power in the two ranges of interest are higher in the fixation task than in the target detection  
 283 task (Friedman non-parametric test, all pairwise comparisons,  $p < 0.001$ ), in agreement with  
 284 the proposal that cognitive flexibility coincides with lower amplitude beta oscillations<sup>52</sup> and  
 285 that attentional engagement coincides with lower amplitude alpha oscillations<sup>53,54</sup>.  
 286 Importantly, these oscillations are absent from the raw MUA signals (Friedman non-  
 287 parametric test, all pairwise comparisons,  $p > 0.2$ ), as well as when noise correlations are  
 288 computed during the same task epochs but from neuronal activities aligned onto target  
 289 presentation (or saccade go signal in the memory guided saccade task, Friedman non-  
 290 parametric test, all pairwise comparisons,  $p > 0.2$ ).

291

292



293

294 **Figure 5: Rhythmic fluctuations in noise correlations modulate behavioral response and**  
 295 **spike-LFP phase coupling in upper input cortical layers.** (A) Single memory guided saccade  
 296 session example of noise correlation variations as a function of trial time. (B) 1/f weighted  
 297 power frequency spectra of noise correlation in time (average  $\pm$  s.e.m), for each task,  
 298 calculated from 300ms to 1500ms from fixation onset (Fixation and Target detection tasks)  
 299 or following cue offset (Memory guided saccade task). (C) Hit rate modulation by alpha (top  
 300 histogram) and beta (bottom histogram) noise correlation at optimal phase as compared to  
 301 anti-optimal phase for all three tasks (color as in (B), average  $\pm$  s.e., dots represent the 95%  
 302 confidence interval under the assumption of absence of behavioral performance phase

303 dependence). (D) Spikes-LFP phase coupling between LFP and spike data as a function of  
304 frequency, time intervals as in (B). (E) Spikes-LFP phase coupling calculated as in (C) but as  
305 a function of the layer attribution of each signal, time intervals as in (B). (F) Average SFC  
306 (+/- s.e.) in alpha (10-16Hz, top histogram) and beta (20-30Hz, bottom histogram) for each  
307 task and both of superficial and deep cortical layer signals (t-test, \*\*\*:  $p < 0.001$ ).

308 Consistent with our previous study<sup>24</sup>, in all of the three tasks, behavioral performance,  
309 defined as the proportion of correct trials as compared to error trials, varied as a function of  
310 alpha and beta noise correlation oscillations. Indeed, on a session by session basis, we could  
311 identify an optimal alpha (10-16Hz) phase for which the behavioral performance was  
312 maximized, in antiphase with a bad alpha phase, for which the behavioral performance was  
313 lowest (figure 5C). These effects were highest in the fixation task (34.6% variation in  
314 behavioral performance) and lowest though significant in the memory-guided saccade task  
315 (13.3% in the target detection task and 9.5% in the memory guided saccade task). Similarly,  
316 an optimal beta (20-30Hz) phase was also found to modulate behavioral performance in the  
317 same range as the observed alpha behavioral modulations (28.3% variation in behavioral  
318 performance in the fixation task, 19.2% in the target detection task and 11% in the memory  
319 guided saccade task). As a result, Alpha and beta oscillation phase in noise correlations were  
320 predictive of behavioral performance, and the strength of these effects co-varied with alpha  
321 and beta oscillation amplitude in noise correlations, being higher in the fixation task, than in  
322 the target detection task than in the memory guided saccade task.

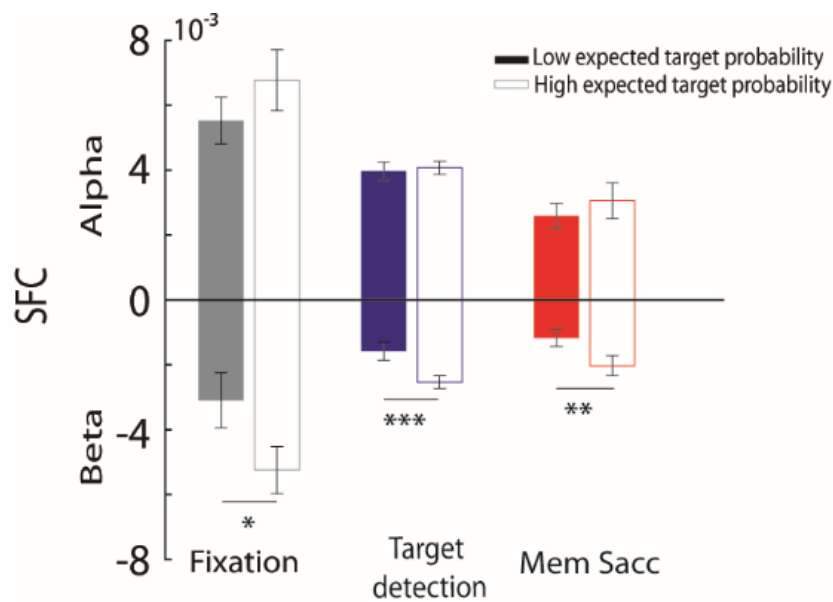
### 323 *Spike-LFP phase coupling (SFC) varies as a function of task demand*

324 In an independent study<sup>24</sup>, we demonstrate that oscillations in noise correlations arise  
325 from specific phase coupling mechanisms between long-range incoming LFP signals and  
326 local spiking mechanisms, independently from phase-amplitude coupling mechanisms. Figure  
327 5D represents SFC between spiking activity and LFP signals (see Materials and Methods)  
328 computed during a 1200ms time interval starting 300ms after either fixation onset (Fixation  
329 and Target detection task) or cue offset (Memory guided saccade task). SFC peaks at both the  
330 frequency ranges identified in the noise correlation spectra, namely the high alpha range (10-  
331 16Hz) and the beta range (20-30Hz). Importantly, this SFC modulation is highest for the  
332 fixation task as compared to the target detection task, thus matching the oscillatory power  
333 differences observed in the noise correlations. SFC are lowest in the memory guided saccade  
334 task whether considering preferred or non-preferred spatial processing. This is probably due  
335 to the fact that the cue to go signal interval of the memory guided saccade task involves

336 memory processes that are expected to desynchronize spiking activity with respect to the LFP  
337 frequencies of interest<sup>46</sup>. This will need to be further explored.

338 In figure 3, we show layer specific effects onto noise correlations that build up onto  
339 the global task effects. An important question is whether these layer effects result from layer  
340 specific changes in SFC. Figure 5E represents the SFC data of figure 5D, segregated on the  
341 bases of the attribution of the MUA to either superficial or deep cortical FEF layers. While  
342 SFC modulations are observed in the same frequencies of interest as in figure 5D, clear layer  
343 specific differences can be observed (figure 5F). Specifically, beta ranges SFC are markedly  
344 significantly lower in the superficial layers than in the deep layers, for both the detection task  
345 and the memory guided saccade task. This points towards a selective control of correlated  
346 noise in input, superficial FEF layers. In contrast, alpha range SFC are significantly lower in  
347 the superficial layers than in the deep layers only in the memory guided saccade, and  
348 specifically when spatial memory is oriented towards a non-preferred location. This points  
349 towards overall weaker layer differences for alpha SFC. Alternatively, alpha SFC could result  
350 from a different mechanism than beta SFC. This will need to be further explored.

351 In figure 4 we show that noise correlations dynamically adjust to the probabilistic  
352 structure of the trial, and are lowest at the time of highest behavioral demand in the trial. In  
353 figure 5D-F, as well as in our independent study<sup>24</sup>, noise correlations and SFC show a strong  
354 pattern of co-variation. We propose that noise correlations arise from specific changes in SFC  
355 coupling. If this is indeed the case, a strong prediction is SFC will also vary as a function of  
356 the probabilistic structure of the task. Figure 6 represents spikes-LFP phase coupling, for each  
357 task, for alpha (upper histogram) and beta (lower histogram) frequency ranges during trials  
358 with both low and high expected response probability. Importantly, only beta ranges SFC are  
359 significantly higher within trials with high expected response probability than in trials with  
360 low expected response probability, and this for all tasks.



361

362 **Figure 6: Spike-LFP phase coupling as a function of expected response probability.**  
363 Average SFC (+/- s.e.) in alpha (10-16Hz, top histogram) and beta (20-30Hz, bottom  
364 histogram) for each task and for both trials with low (filled bars) and high (empty bars)  
365 expected response probability (t-test, \*\*\*:  $p < 0.001$ ).

## 366 Discussion

367 In this work, our main goal was to examine the impact of cognitive engagement and  
368 task demands onto the neuronal population shared variability as assessed from inter-neuronal  
369 noise correlations at multiple time scales. Recordings were performed in the macaque frontal  
370 eye fields, a cortical region in which neuronal noise correlations have been shown to vary as a  
371 function of spatial attention<sup>25</sup> and spatial memory<sup>26,55</sup>. Noise correlations were computed over  
372 equivalent behavioral task epochs, prior to response production, during a delay in which eyes  
373 were fixed and in the absence of any intervening sensory event or motor response. As a result,  
374 any observed differences in noise correlations are to be assigned to an endogenous source of  
375 shared neuronal variability.

376 Overall, we demonstrate, for the first time, that noise correlations dynamically adjust  
377 to task demands at different time scales. Specifically, we show that noise correlations  
378 decrease as cognitive engagement and task demands increase. These task-related variations in  
379 noise correlations co-exist with within-trial dynamic changes related to the probabilistic  
380 structure of the tasks as well as with long- and short-range oscillatory brain mechanisms.

381 ***Shared neuronal population response variability dynamically adjusts to the***  
382 ***behavioral demands.***

383 Noise correlations have been shown to vary with learning or changes in behavioral  
384 state (V1<sup>56-59</sup>, V4<sup>25,60-62</sup> and MT<sup>4,63,64</sup>). For example, shared neuronal population response

385 variability was lower in V1 in trained than in naïve monkeys<sup>27</sup>. More recently, Ni et al.  
386 describe, within visual areas, a robust relationship between correlated variability and  
387 perceptual performance, whether changes in performance happened rapidly (attention  
388 instructed by a spatial cue) or slowly (learning). This relationship was robust even when the  
389 main effects of attention and learning were accounted for<sup>28</sup>. Here, we question whether  
390 changes in noise correlations can be observed simultaneously at multiple time scales. We  
391 describe two different times scales at which noise correlations dynamically adjust to the task  
392 demands.

393 The first adjustment in noise correlations we describe is between tasks, that is between  
394 blocked contexts of varying cognitive demand, the monkeys knowing that general task  
395 requirements will be constant over a hundred of trials or more. Task performance is taken as a  
396 proxy to cognitive adjustment to the task demands and negatively correlates with noise  
397 correlations in the recorded population. Shared neuronal population variability measure is  
398 largest in the fixation task as compared to the two other tasks, by almost 30%. The difference  
399 between noise correlations in the target detection task as compared to the guided memory  
400 saccade task is in the range of 2%, closer to what has been previously reported in the context  
401 of noise correlation changes under spatial attention<sup>25</sup> or spatial memory manipulations.  
402 Importantly, these changes in noise correlations are observed in the absence of significant  
403 variations in individual neuronal spiking statistics (average spiking rates, spiking variability  
404 or associated Fano factor). To our knowledge, this is the first time that such task effects are  
405 described onto noise correlations. This variation in noise correlations as a function of  
406 cognitive engagement and task requirements suggests an adaptive mechanism that adjusts  
407 noise correlations to the ongoing behavior. Such a mechanism is expected to express itself at  
408 different timescales, ranging from the task level, to the across trial level to the within trial  
409 level. This is explored next.

410 It is unclear whether the transitions between high and low noise correlation states  
411 when changing from one task to another are fast (over one or two trials) or slow (over tens of  
412 trials). In<sup>51</sup>, we show that noise correlations vary as a function of immediate trial past history.  
413 Specifically, noise correlations are significantly higher on error trials than on correct trials,  
414 both measures being higher if the previous trial is an error trial than if the previous trial is a  
415 correct trial. We thus predict a similar past history effect to be observed on noise correlations  
416 at transitions between tasks, and we expect for example, noise correlations to be lower in  
417 fixation trials that are preceded by a target detection trial, than in trials preceded by fixation

418 trials. In our experimental design, task transitions are unfortunately rare events, precluding the  
419 computation of noise correlations on these transitions.

420 However, our experimental design affords an analysis at a much finer timescale, i.e.  
421 the description of a dynamical adjustment in noise correlations within trials. Specifically, we  
422 show that noise correlations dynamically adjust to the probability of occurrence of a  
423 behaviorally key task event associated with the reward response production (target  
424 presentation on the fixation and target detection tasks or saccade go signal on the memory  
425 guided saccade task). In other words, shared neuronal population response variability  
426 dynamically adjusts to higher demand task epochs. As expected from the general idea that low  
427 noise correlations allow for optimal signal processing<sup>12,65,66</sup>, we show that, on each of the  
428 three tasks, at any given time in the fixation epoch prior to response production, the higher the  
429 probability of having to initiate a response, the lower the noise correlations.

430 Overall, this supports the idea that noise correlations is a flexible physiological  
431 parameter that dynamically adjusts at multiple timescales to optimally meet ongoing  
432 behavioral demands, as has been demonstrated in multisensory integration<sup>67</sup> and through  
433 learning and attention<sup>28</sup>. The mechanisms through which this possibly takes place are  
434 discussed below.

#### 435 *Rhythmic fluctuations in noise correlations.*

436 In the above, we describe changes in noise correlations between tasks as a function of  
437 the cognitive demand, as well as within trials, as a function of the probabilistic structure of  
438 each task. In addition to these task-related dynamics, we also confirm our concurrent  
439 observation of rhythmic fluctuations in noise correlations<sup>24</sup>. These fluctuations are clearly  
440 identified in the high alpha frequency range (10-16 Hz) and to a lesser extent in the low  
441 gamma frequency range (20-30Hz). To our knowledge, this is the first time that such  
442 rhythmic variations in noise correlations are reported. The question is whether these  
443 oscillations have a functional relevance or not.

444 From a behavioral point of view, we show that overt behavioral performance in the  
445 three tasks co-varies with both the 10-16Hz and 20-30Hz noise correlation oscillations. In  
446 other words, these oscillations account for more than 10% of the behavioral response  
447 variability, strongly supporting a functional role for these alpha and beta oscillations.

448 From a functional point of view, attention directed to the receptive field of neurons has  
449 been shown to both reduce noise correlations<sup>24</sup> and spike-field coherence in the gamma range  
450 (V4<sup>68</sup>, it is however to be noted that Engel et al. describe increased spike-field coherence in

451 V1, the gamma range under the same conditions, hinting towards areal specific differences<sup>69</sup>).  
452 In our hands, both the rhythmic fluctuations in noise correlations and the task and trial-related  
453 changes in noise correlations co-exist with increased spike-LFP phase coupling in the very  
454 same 10-16Hz and/or 20-30Hz frequency ranges we identify in the noise correlations. This  
455 suggests that changes in shared neuronal variability possibly arise from changes in the local  
456 coupling between neuronal spiking activity and local field potentials. Supporting such a  
457 functional coupling, both the observed changes in noise correlations and spike-LFP phase  
458 coupling in the frequencies of interest are highest in the fixation task as compared to the other  
459 two tasks.

460 Beta oscillations in the local field potentials (LFP) are considered to reflect long-range  
461 processes and have been associated with cognitive control and flexibility<sup>29,52,69-72</sup> as well as  
462 with motor control<sup>73-75</sup>( for review see<sup>52</sup>). Specifically, lower beta power LFPs has been  
463 associated with states of higher cognitive flexibility. In our hands, lower beta in noise  
464 correlations correspond to higher cognitive demands. We thus hypothesize a functional link  
465 between these two measures, LFP oscillations locally changing spiking statistics, i.e. noise  
466 correlations, by a specific spike-LFP phase coupling in this frequency range. Supporting a  
467 long-range origin of these local processes (figure 7, inset), we show that spike-LFP phase  
468 coupling in this beta range strongly decreases in the more superficial cortical layers as  
469 compared to the deeper layers, as task cognitive demand increases. On the other hand, alpha  
470 oscillations are associated with attention, anticipation<sup>53,54</sup>, perception<sup>76-78</sup>, and working  
471 memory<sup>79</sup>. As for beta oscillations, lower alpha in noise correlations, and accordingly in  
472 spike-LFP phase coupling, correspond to higher cognitive demands. In contrast with what is  
473 observed for beta spike-LFP phase coupling, alpha spike-LFP phase coupling does not exhibit  
474 any layer specificity across task demands. Thus overall, alpha and beta rhythmicity account  
475 for strong fluctuations in behavioral performance, as well as for changes in spike-LFP phase  
476 coupling. However, beta processes seem to play a distinct functional role as compared to the  
477 alpha processes, as their effect is more marked in the superficial than in the deeper cortical  
478 layers. These observations coincide with recent evidence that cognition is rhythmic<sup>80,81,87</sup> and  
479 that noise correlations play a key role in optimizing behavior to the ongoing time-varying  
480 cognitive demands<sup>27</sup>.

481

482

483 ***Acknowledgments***

484 S.B.H.H. was supported by ANR grant ANR-14-CE13-0005-1. C.G. was supported by the  
485 French Ministère de l'Enseignement Supérieur et de la Recherche. S.B.H. was supported by  
486 ANR grant ANR-11-BSV4-0011, ANR grant ANR-14-CE13-0005-1, and the LABEX  
487 CORTEX (ANR-11-LABX-0042) of Université de Lyon, within the program Investissements  
488 d'Avenir (ANR-11-IDEX-0007) operated by the French National Research Agency (ANR).  
489 E.A. was supported by the CNRS-DGA and Fondation pour la Recherche Médicale. We thank  
490 research engineer Serge Pinède for technical support and Jean-Luc Charieau and Fabrice  
491 Hérant for animal care. All procedures were approved by the local animal care committee  
492 (C2EA42-13-02-0401-01) in compliance with the European Community Council, Directive  
493 2010/63/UE on Animal Care.

494

495 ***Authors contributions***

496 Conceptualization, S.B.H. S.B.H.H. and C.G.; Methodology, S.B.H., S.B.H.H., C.G., E.A.,  
497 C.W.; Investigation, S.B.H., S.B.H.H., C.G., E.A. and C.W.; Writing – Original Draft, S.B.H.  
498 S.B.H.H. and C.G.; Writing – Review & Editing, S.B.H. S.B.H.H. and C.G.; Funding  
499 Acquisition, S.B.H.; Supervision, S.B.H.

500

501 **References**

- 502 1. Ts'o, D. Y., Gilbert, C. D. & Wiesel, T. N. Relationships between horizontal interactions  
503 and functional architecture in cat striate cortex as revealed by cross-correlation analysis.  
504 *J. Neurosci.* **6**, 1160–1170 (1986).
- 505 2. Engel, A. K., König, P., Kreiter, A. K. & Singer, W. Interhemispheric Synchronization of  
506 Oscillatory Neuronal Responses in Cat Visual Cortex. *Science.* **252**, 1177–1179 (1991).
- 507 3. Ahissar, E. *et al.* Dependence of Cortical Plasticity on Correlated Activity of Single  
508 Neurons and on Behavioral Context. *Science.* **257**, 1412–1415 (1992).
- 509 4. Zohary, E., Shadlen, M. N. & Newsome, W. T. Correlated neuronal discharge rate and its  
510 implications for psychophysical performance. *Nature.* **370**, 140–143 (1994).
- 511 5. Vaadia, E. *et al.* Dynamics of neuronal interactions in monkey cortex in relation to  
512 behavioural events. *Nature.* **373**, 515–518 (1995).
- 513 6. Narayanan, N. S. & Laubach, M. Top-down control of motor cortex ensembles by  
514 dorsomedial prefrontal cortex. *Neuron.* **52**, 921–931 (2006).
- 515 7. Cohen, J. Y. *et al.* Cooperation and competition among frontal eye field neurons during  
516 visual target selection. *J. Neurosci. Off. J. Soc. Neurosci.* **30**, 3227–3238 (2010).
- 517 8. Poulet, J. F. A. & Petersen, C. C. H. Internal brain state regulates membrane potential  
518 synchrony in barrel cortex of behaving mice. *Nature.* **454**, 881–885 (2008).
- 519 9. Stark, E., Globerson, A., Asher, I. & Abeles, M. Correlations between groups of premotor  
520 neurons carry information about prehension. *J. Neurosci. Off. J. Soc. Neurosci.* **28**,  
521 10618–10630 (2008).
- 522 10. Abbott, L. F. & Dayan, P. *The Effect of Correlated Variability on the Accuracy of a*  
523 *Population Code.* *Neural Computation.* **11**, 91-101 (1999).
- 524 11. Sompolinsky, H., Yoon, H., Kang, K. & Shamir, M. Population coding in neuronal  
525 systems with correlated noise. *Phys. Rev. E Stat. Nonlin. Soft Matter Phys.* **64**, 051904  
526 (2001).
- 527 12. Averbeck, B. B., Latham, P. E. & Pouget, A. Neural correlations, population coding and  
528 computation. *Nat. Rev. Neurosci.* **7**, 358–366 (2006).
- 529 13. Ecker, A. S., Berens, P., Tolias, A. S. & Bethge, M. The effect of noise correlations in  
530 populations of diversely tuned neurons. *J. Neurosci.* **31**, 14272-14283 (2011)
- 531 14. Moreno-Bote, R. *et al.* Information-limiting correlations. *Nat. Neurosci.* **17**, 1410 (2014).
- 532 15. Ekstrom, L. B., Roelfsema, P. R., Arsenault, J. T., Bonmassar, G. & Vanduffel, W.  
533 Bottom-up dependent gating of frontal signals in early visual cortex. *Science.* **321**, 414–  
534 417 (2008).

- 535 16. Shadlen, M. N. & Newsome, W. T. The variable discharge of cortical neurons:  
536 implications for connectivity, computation, and information coding. *J. Neurosci. Off. J.*  
537 *Soc. Neurosci.* **18**, 3870–3896 (1998).
- 538 17. Ecker, A. S. *et al.* State Dependence of Noise Correlations in Macaque Primary Visual  
539 Cortex. *Neuron*. **82**, 235–248 (2014).
- 540 18. Goris, R. L. T., Movshon, J. A. & Simoncelli, E. P. Partitioning neuronal variability. *Nat.*  
541 *Neurosci.* **17**, 858–865 (2014).
- 542 19. Wimmer, K. *et al.* Sensory integration dynamics in a hierarchical network explains choice  
543 probabilities in cortical area MT. *Nat. Commun.* **6**, 6177 (2015).
- 544 20. Ben-Yishai, R., Bar-Or, R. L. & Sompolinsky, H. Theory of orientation tuning in visual  
545 cortex. *Proc. Natl. Acad. Sci. U. S. A.* **92**, 3844–3848 (1995).
- 546 21. Litwin-Kumar, A. & Doiron, B. Slow dynamics and high variability in balanced cortical  
547 networks with clustered connections. *Nat. Neurosci.* **15**, 1498–1505 (2012).
- 548 22. Ly, C., Middleton, J. W. & Doiron, B. Cellular and circuit mechanisms maintain low  
549 spike co-variability and enhance population coding in somatosensory cortex. *Front.*  
550 *Comput. Neurosci.* **6**, 7 (2012).
- 551 23. Kanitscheider, I., Coen-Cagli, R. & Pouget, A. Origin of information-limiting noise  
552 correlations. *Proc. Natl. Acad. Sci. U. S. A.* **112**, E6973–6982 (2015).
- 553 24. Ben Hadj Hassen, S., Gaillard, C., Astrand, E., Wardak, C. & Ben Hamed, S. Rhythmic  
554 variations in prefrontal inter-neuronal correlations, their underlying mechanisms and their  
555 behavioral correlates. *bioRxiv* 784850 (2019)
- 556 25. Cohen, M. R. & Maunsell, J. H. R. Attention improves performance primarily by  
557 reducing interneuronal correlations. *Nat. Neurosci.* **12**, 1594–1600 (2009).
- 558 26. Meyers, E. M., Qi, X.-L. & Constantinidis, C. Incorporation of new information into  
559 prefrontal cortical activity after learning working memory tasks. *Proc. Natl. Acad. Sci. U.*  
560 *S. A.* **109**, 4651–4656 (2012).
- 561 27. Gu, Y. *et al.* Perceptual learning reduces interneuronal correlations in macaque visual  
562 cortex. *Neuron*. **71**, 750–761 (2011).
- 563 28. Ni, A. M., Ruff, D. A., Alberts, J. J., Symmonds, J. & Cohen, M. R. Learning and  
564 attention reveal a general relationship between population activity and behavior. *Science.*  
565 **359**, 463–465 (2018).
- 566 29. Buschman, T. J. & Miller, E. K. Top-down versus bottom-up control of attention in the  
567 prefrontal and posterior parietal cortices. *Science.* **315**, 1860–1862 (2007).

- 568 30. Wardak, C., Ibos, G., Duhamel, J.-R. & Olivier, E. Contribution of the monkey frontal  
569 eye field to covert visual attention. *J. Neurosci. Off. J. Soc. Neurosci.* **26**, 4228–4235  
570 (2006).
- 571 31. Ibos, G., Duhamel, J.-R. & Ben Hamed, S. A functional hierarchy within the  
572 parietofrontal network in stimulus selection and attention control. *J. Neurosci. Off. J. Soc.*  
573 *Neurosci.* **33**, 8359–8369 (2013).
- 574 32. Gregoriou, G. G., Gotts, S. J., Zhou, H. & Desimone, R. High-frequency, long-range  
575 coupling between prefrontal and visual cortex during attention. *Science.* **324**, 1207–1210  
576 (2009).
- 577 33. Gregoriou, G. G., Gotts, S. J. & Desimone, R. Cell-type-specific synchronization of  
578 neural activity in FEF with V4 during attention. *Neuron.* **73**, 581–594 (2012).
- 579 34. Armstrong, K. M., Chang, M. H. & Moore, T. Selection and maintenance of spatial  
580 information by frontal eye field neurons. *J. Neurosci. Off. J. Soc. Neurosci.* **29**, 15621–  
581 15629 (2009).
- 582 35. Schölvinck, M. L., Saleem, A. B., Benucci, A., Harris, K. D. & Carandini, M. Cortical  
583 state determines global variability and correlations in visual cortex. *J. Neurosci. Off. J.*  
584 *Soc. Neurosci.* **35**, 170–178 (2015).
- 585 36. Arieli, A., Sterkin, A., Grinvald, A. & Aertsen, A. Dynamics of ongoing activity:  
586 explanation of the large variability in evoked cortical responses. *Science.* **273**, 1868–1871  
587 (1996).
- 588 37. Bair, W., Zohary, E. & Newsome, W. T. Correlated firing in macaque visual area MT:  
589 time scales and relationship to behavior. *J. Neurosci. Off. J. Soc. Neurosci.* **21**, 1676–1697  
590 (2001).
- 591 38. Bryant, H. L., Marcos, A. R. & Segundo, J. P. Correlations of neuronal spike discharges  
592 produced by monosynaptic connections and by common inputs. *J. Neurophysiol.* **36**, 205–  
593 225 (1973).
- 594 39. Bruce, C. J. & Goldberg, M. E. Primate frontal eye fields: I. Single neurons discharging  
595 before saccades. *J. Neurophysiol.* **53**, 603 (1985).
- 596 40. Astrand, E., Ibos, G., Duhamel, J.-R. & Ben Hamed, S. Differential dynamics of spatial  
597 attention, position, and color coding within the parietofrontal network. *J. Neurosci. Off. J.*  
598 *Soc. Neurosci.* **35**, 3174–3189 (2015).
- 599 41. Segraves, M. A. & Goldberg, M. E. Functional properties of corticotectal neurons in the  
600 monkey's frontal eye field. *J. Neurophysiol.* **58**, 1387–1419 (1987).

- 601 42. Schall, J. D. Neuronal activity related to visually guided saccades in the frontal eye fields  
602 of rhesus monkeys: comparison with supplementary eye fields. *J. Neurophysiol.* **66**, 559–  
603 579 (1991).
- 604 43. Schall, J. D. & Hanes, D. P. Neural basis of saccade target selection in frontal eye field  
605 during visual search. *Nature.* **366**, 467–469 (1993).
- 606 44. Schall, J. D., Hanes, D. P., Thompson, K. G. & King, D. J. Saccade target selection in  
607 frontal eye field of macaque. I. Visual and premovement activation. *J. Neurosci. Off. J.*  
608 *Soc. Neurosci.* **15**, 6905–6918 (1995).
- 609 45. Schall, J. D. & Thompson, K. G. Neural selection and control of visually guided eye  
610 movements. *Annu. Rev. Neurosci.* **22**, 241–259 (1999).
- 611 46. Buffalo, E. A., Fries, P., Landman, R., Buschman, T. J. & Desimone, R. Laminar  
612 differences in gamma and alpha coherence in the ventral stream. *Proc. Natl. Acad. Sci. U.*  
613 *S. A.* **108**, 11262–11267 (2011).
- 614 47. Womelsdorf, T., Fries, P., Mitra, P. P. & Desimone, R. Gamma-band synchronization in  
615 visual cortex predicts speed of change detection. *Nature.* **439**, 733–736 (2006).
- 616 48. Womelsdorf, T., Anton-Erxleben, K. & Treue, S. Receptive field shift and shrinkage in  
617 macaque middle temporal area through attentional gain modulation. *J. Neurosci. Off. J.*  
618 *Soc. Neurosci.* **28**, 8934–8944 (2008).
- 619 49. Anton-Erxleben, K., Henrich, C. & Treue, S. Attention changes perceived size of moving  
620 visual patterns. *J. Vis.* **7**, 5.1-9 (2007).
- 621 50. Ben Hamed, S., Duhamel, J.-R., Bremmer, F. & Graf, W. Visual receptive field  
622 modulation in the lateral intraparietal area during attentive fixation and free gaze. *Cereb.*  
623 *Cortex N. Y. N.* **12**, 234–245 (2002).
- 624 51. Astrand, E., Wardak, C., Baraduc, P. & Ben Hamed, S. Direct Two-Dimensional Access  
625 to the Spatial Location of Covert Attention in Macaque Prefrontal Cortex. *Curr. Biol. CB*  
626 **26**, 1699–1704 (2016).
- 627 52. Engel, A. K. & Fries, P. Beta-band oscillations--signalling the status quo? *Curr. Opin.*  
628 *Neurobiol.* **20**, 156–165 (2010).
- 629 53. Thut, G., Nietzel, A., Brandt, S. A. & Pascual-Leone, A. Alpha-band  
630 electroencephalographic activity over occipital cortex indexes visuospatial attention bias  
631 and predicts visual target detection. *J. Neurosci. Off. J. Soc. Neurosci.* **26**, 9494–9502  
632 (2006).

- 633 54. Rihs, T. A., Michel, C. M. & Thut, G. A bias for posterior alpha-band power suppression  
634 versus enhancement during shifting versus maintenance of spatial attention. *NeuroImage*  
635 **44**, 190–199 (2009).
- 636 55. Constantinidis, C. & Klingberg, T. The neuroscience of working memory capacity and  
637 training. *Nat. Rev. Neurosci.* **17**, 438–449 (2016).
- 638 56. Smith, M. A. & Kohn, A. Spatial and Temporal Scales of Neuronal Correlation in  
639 Primary Visual Cortex. *J. Neurosci.* **28**, 12591–12603 (2008).
- 640 57. Gutnisky, D. A. & Dragoi, V. Adaptive coding of visual information in neural  
641 populations. *Nature.* **452**, 220–224 (2008).
- 642 58. Poort, J. & Roelfsema, P. R. Noise correlations have little influence on the coding of  
643 selective attention in area V1. *Cereb. Cortex N. Y. N 1991.* **19**, 543–553 (2009).
- 644 59. Reich, D. S. Independent and Redundant Information in Nearby Cortical Neurons.  
645 *Science.* **294**, 2566–2568 (2001).
- 646 60. Mitchell, J. F., Sundberg, K. A. & Reynolds, J. H. Spatial attention decorrelates intrinsic  
647 activity fluctuations in macaque area V4. *Neuron.* **63**, 879–888 (2009).
- 648 61. Gawne, T. J., Kjaer, T. W., Hertz, J. A. & Richmond, B. J. Adjacent visual cortical  
649 complex cells share about 20% of their stimulus-related information. *Cereb. Cortex N. Y.*  
650 *N 1991.* **6**, 482–489 (1996).
- 651 62. Gawne, T. J. & Richmond, B. J. How independent are the messages carried by adjacent  
652 inferior temporal cortical neurons? *J. Neurosci. Off. J. Soc. Neurosci.* **13**, 2758–2771  
653 (1993).
- 654 63. Cohen, M. R. & Newsome, W. T. Context-dependent changes in functional circuitry in  
655 visual area MT. *Neuron.* **60**, 162–173 (2008).
- 656 64. Huang, X. & Lisberger, S. G. Noise Correlations in Cortical Area MT and Their Potential  
657 Impact on Trial-by-Trial Variation in the Direction and Speed of Smooth-Pursuit Eye  
658 Movements. *J. Neurophysiol.* **101**, 3012–3030 (2009).
- 659 65. Ecker, A. S. *et al.* Decorrelated Neuronal Firing in Cortical Microcircuits. *Science.* **327**,  
660 584–587 (2010).
- 661 66. Renart, A. *et al.* The asynchronous state in cortical circuits. *Science.* **327**, 587–590  
662 (2010).
- 663 67. Chandrasekaran, C. Computational principles and models of multisensory integration.  
664 *Curr. Opin. Neurobiol.* **43**, 25–34 (2017).
- 665 68. Chalk, M. *et al.* Attention Reduces Stimulus-Driven Gamma Frequency Oscillations and  
666 Spike Field Coherence in V1. *Neuron.* **66**, 114 (2010).

- 667 69. Engel, A. K., Fries, P. & Singer, W. Dynamic predictions: oscillations and synchrony in  
668 top-down processing. *Nat. Rev. Neurosci.* **2**, 704–716 (2001).
- 669 70. Okazaki, M., Kaneko, Y., Yumoto, M. & Arima, K. Perceptual change in response to a  
670 bistable picture increases neuromagnetic beta-band activities. *Neurosci. Res.* **61**, 319–328  
671 (2008).
- 672 71. Iversen, J. R., Repp, B. H. & Patel, A. D. Top-down control of rhythm perception  
673 modulates early auditory responses. *Ann. N. Y. Acad. Sci.* **1169**, 58–73 (2009).
- 674 72. Buschman, T. J. & Miller, E. K. Serial, covert shifts of attention during visual search are  
675 reflected by the frontal eye fields and correlated with population oscillations. *Neuron.* **63**,  
676 386–396 (2009).
- 677 73. Joundi, R. A., Jenkinson, N., Brittain, J.-S., Aziz, T. Z. & Brown, P. Driving oscillatory  
678 activity in the human cortex enhances motor performance. *Curr. Biol. CB.* **22**, 403–407  
679 (2012).
- 680 74. Lalo, E. *et al.* Phasic increases in cortical beta activity are associated with alterations in  
681 sensory processing in the human. *Exp. Brain Res.* **177**, 137–145 (2007).
- 682 75. Courtemanche, R., Fujii, N. & Graybiel, A. M. Synchronous, focally modulated beta-band  
683 oscillations characterize local field potential activity in the striatum of awake behaving  
684 monkeys. *J. Neurosci. Off. J. Soc. Neurosci.* **23**, 11741–11752 (2003).
- 685 76. Varela, F. J., Toro, A., John, E. R. & Schwartz, E. L. Perceptual framing and cortical  
686 alpha rhythm. *Neuropsychologia.* **19**, 675–686 (1981).
- 687 77. Mathewson, K. E., Gratton, G., Fabiani, M., Beck, D. M. & Ro, T. To See or Not to See:  
688 Prestimulus  $\alpha$  Phase Predicts Visual Awareness. *J. Neurosci.* **29**, 2725–2732 (2009).
- 689 78. Busch, N. A. & VanRullen, R. Spontaneous EEG oscillations reveal periodic sampling of  
690 visual attention. *Proc. Natl. Acad. Sci. U. S. A.* **107**, 16048–16053 (2010).
- 691 79. Klimesch, W. EEG-alpha rhythms and memory processes. *Int. J. Psychophysiol. Off. J.*  
692 *Int. Organ. Psychophysiol.* **26**, 319–340 (1997).
- 693 80. Fiebelkorn, I. C., Pinsk, M. A. & Kastner, S. A Dynamic Interplay within the  
694 Frontoparietal Network Underlies Rhythmic Spatial Attention. *Neuron.* **99**, 842-853.e8  
695 (2018).
- 696 81. Fiebelkorn, I. C. & Kastner, S. A Rhythmic Theory of Attention. *Trends Cogn. Sci.*  
697 **11.009** (2018).
- 698 82. Oostenveld, R., Fries, P., Maris, E. & Schoffelen, J.-M. FieldTrip: Open Source Software  
699 for Advanced Analysis of MEG, EEG, and Invasive Electrophysiological Data. *Intell*  
700 *Neurosci.* **2011**, 1:1–1:9 (2011).

- 701 83. Grinsted, A., Moore, J. C. & Jevrejeva, S. Application of the cross wavelet transform and  
702 wavelet coherence to geophysical time series. *Nonlinear Process. Geophys.* **11**, 561–566  
703 (2004).
- 704 84. Buffalo, E. A., Fries, P., Landman, R., Buschman, T. J. & Desimone, R. Laminar  
705 differences in gamma and alpha coherence in the ventral stream. *Proc. Natl. Acad. Sci. U.*  
706 *S. A.* **108**, 11262–11267 (2011).
- 707 85. Cohen, M. R. & Maunsell, J. H. R. Attention improves performance primarily by  
708 reducing interneuronal correlations. *Nat. Neurosci.* **12**, 1594–1600 (2009).
- 709 86. Fiebelkorn, I. C. *et al.* Cortical cross-frequency coupling predicts perceptual outcomes.  
710 *NeuroImage* **69**, 126–137 (2013).
- 711 87. Gaillard, C., Ben Hadj Hassen, S., Di Bello, F., Bihan-Poudec, Y., VanRullen, R., Ben  
712 Hamed, S. Prefrontal attentional saccades explore space at an alpha rhythm. *bioRxiv*  
713 637975 (2019). doi:10.1101/637975
- 714
- 715

## 716 **Supplementary material and methods**

### 717 **Material and methods**

#### 718 **Ethical statement**

719 All procedures were in compliance with the guidelines of European Community on  
720 animal care (Directive 2010/63/UE of the European Parliament and the Council of 22  
721 September 2010 on the protection of animals used for scientific purposes) and authorized by  
722 the French Committee on the Ethics of Experiments in Animals (C2EA) CELYNE registered  
723 at the national level as C2EA number 42 (protocole C2EA42-13-02-0401-01).

#### 724 **Surgical procedure**

725 As in<sup>51</sup>, two male rhesus monkeys (*Macaca mulatta*) weighing between 6-8 kg  
726 underwent a unique surgery during which they were implanted with two MRI compatible  
727 PEEK recording chambers placed over the left and the right FEF hemispheres respectively  
728 (figure 1A), as well as a head fixation post. Gas anesthesia was carried out using Vet-Flurane,  
729 0.5 – 2% (Isofluranum 100%) following an induction with Zolétil 100 (Tiletamine at  
730 50mg/ml, 15mg/kg and Zolazepam, at 50mg/ml, 15mg/kg). Post-surgery pain was controlled  
731 with a morphine pain-killer (Buprecare, buprenorphine at 0.3mg/ml, 0.01mg/kg), 3 injections  
732 at 6 hours interval (first injection at the beginning of the surgery) and a full antibiotic  
733 coverage was provided with Baytril 5% (a long action large spectrum antibiotic, Enrofloxacin  
734 0.5mg/ml) at 2.5mg/kg, one injection during the surgery and thereafter one each day during  
735 10 days. A 0.6mm isomorphic anatomical MRI scan was acquired post surgically on a 1.5T  
736 Siemens Sonata MRI scanner, while a high-contrast oil filled grid (mesh of holes at a  
737 resolution of 1mmx1mm) was placed in each recording chamber, in the same orientation as  
738 the final recording grid. This allowed a precise localization of the arcuate sulcus and  
739 surrounding gray matter underneath each of the recording chambers. The FEF was defined as  
740 the anterior bank of the arcuate sulcus and we specifically targeted those sites in which a  
741 significant visual and/or oculomotor activity was observed during a memory guided saccade  
742 task at 10 to 15° of eccentricity from the fixation point (figure 1A). In order to maximize task-  
743 related neuronal information at each of the 24-contacts of the recording probes, we only  
744 recorded from sites with task-related activity observed continuously over at least 3 mm of  
745 depth.

#### 746 **Behavioral task**

747 During a given experimental session, the monkeys were placed in front of a computer screen  
748 (1920x1200 pixels and a refresh rate of 60 Hz) with their head fixed. Their water intake was  
749 controlled so that their initial daily intake was covered by their performance in the task, on a  
750 trial by trial basis. This quantity was complemented as follows. On good performance  
751 sessions, monkeys received fruit and water complements. On bad performance sessions, water  
752 complements were provided at a distance from the end of the session. Each recording session  
753 consisted of random alternations of three different tasks (see below and figure 1B), so as to  
754 control for possible time in the session or task order effects. For all tasks, to initiate a trial, the  
755 monkeys had to hold a bar in front of the animal chair, thus interrupting an infrared beam. (1)  
756 **Fixation Task** (figure 1B.1): A red fixation cross ( $0.7 \times 0.7^\circ$ ), appeared in the center of the  
757 screen and the monkeys were required to hold fixation during a variable interval randomly  
758 ranging between 7000 and 9500ms, within a fixation window of  $1.5 \times 1.5^\circ$ , until the color  
759 change of the central cross. At this time, the monkeys had to release the bar within 150-800  
760 ms after color change. Success conditioned reward delivery. (2) **Target detection Task** (figure  
761 1B.2): A red fixation cross ( $0.7 \times 0.7^\circ$ ), appeared in the center of the screen and the monkeys  
762 were required to hold fixation during a variable interval ranging between 1300 and 3400 ms,  
763 within a fixation window of  $1.5 \times 1.5^\circ$ , until a green squared target ( $0.28 \times 0.28^\circ$ ) was presented  
764 for 100 ms in one of four possible positions ( $(10^\circ, 10^\circ)$ ,  $(-10^\circ, 10^\circ)$ ,  $(-10^\circ, -10^\circ)$  and  $(10^\circ, -10^\circ)$ )  
765 in a randomly interleaved order. At this time, the monkeys had to release the bar within 150-  
766 800 ms after target onset. Success conditioned reward delivery. (3) **Memory-guided saccade**  
767 **Task** (figure 1B.3): A red fixation cross ( $0.7 \times 0.7^\circ$ ) appeared in the center of the screen and  
768 the monkeys were required to hold fixation for 500 msec, within a fixation window of  
769  $1.5 \times 1.5^\circ$ . A squared green cue ( $0.28 \times 0.28^\circ$ ) was then flashed for 100ms at one of four  
770 possible locations ( $(10^\circ, 10^\circ)$ ,  $(-10^\circ, 10^\circ)$ ,  $(-10^\circ, -10^\circ)$  and  $(10^\circ, -10^\circ)$ ). The monkeys had to  
771 continue maintain fixation on the central fixation point for another 700-1900 ms until the  
772 fixation point disappeared. The monkeys were then required to make a saccade towards the  
773 memorized location of the cue within 500-800ms from fixation point disappearance, and a  
774 spatial tolerance of  $4^\circ \times 4^\circ$ . On success, a target, identical to the cue was presented at the cued  
775 location and the monkeys were required to fixate it and detect a change in its color by a bar  
776 release within 150-800 ms from color change. Success in all of these successive requirements  
777 conditioned reward delivery.

## 778 **Neural recordings**

779 On each session, bilateral simultaneous recordings in the two FEFs were carried out  
780 using two 24- contacts Plexon U-probes. The contacts had an interspacing distance of 250  
781  $\mu\text{m}$ . Neural data was acquired with the Plexon Omniplex® neuronal data acquisition system.  
782 The data was amplified 400 times and digitized at 40,000 Hz. The MUA neuronal data was  
783 high-pass filtered at 300 Hz. The LFP neuronal data was filtered between 0.5 and 300 Hz. In  
784 the present paper, all analyses are performed on the multi-unit activity recorded on each of the  
785 48 recording contacts. A threshold defining the multi-unit activity was applied independently  
786 for each recording contact and before the actual task-related recordings started. All further  
787 analyses of the data were performed in Matlab™ and using FieldTrip<sup>82</sup> and the Wavelet  
788 Coherence Matlab Toolbox<sup>83</sup>, both open source Matlab™ toolboxes.

## 789 **Data Analysis**

790 **Data preprocessing.** Overall, MUA recordings were collected from 48 recording  
791 channels on 26 independent recording sessions (13 for M1 and 13 for M2). We excluded from  
792 subsequent analyses all channels with less than 5 spikes per seconds. For each session, we  
793 identified the task-related channels based on a statistical change (one-way ANOVA,  $p < 0.05$ )  
794 in the MUA neuronal activity in the memory-guided saccade task, in response to either cue  
795 presentation ([0 400] ms after cue onset) against a pre-cue baseline ([-100 0] ms relative to  
796 cue onset), or to saccade execution go signal and to saccade execution (i.e. fixation point off,  
797 [0 400] ms after go signal) against a pre-go signal baseline ([-100 0] ms relative to go signal),  
798 irrespective of the spatial configuration of the trial. In total, 671 channels were retained for  
799 further analyses out of 1248 channels.

800 **MUA spatial selectivity.** FEF neurons are characterized by a strong visual, saccadic,  
801 spatial memory and spatial attention selectivity<sup>30,38,39</sup>. We used a one-way ANOVA ( $p < 0.05$ )  
802 to identify the spatially selective channels in response to cue presentation ([0 400] ms  
803 following cue onset) and to the saccade execution go signal ([0 400] ms following go signal).  
804 Post-hoc t-tests served to further order, for each channels, the neuron's response in each  
805 visual quadrant from preferred (p1), to least preferred (p4). By convention, positive  
806 modulations were considered as preferred and negative modulations as least preferred. For  
807 example, in a given session, the MUA signal recorded on channel 1 of a probe placed in the  
808 left FEF, could have as best preferred position p1 the upper right quadrant, the next best  
809 preferred position p2 the lower right quadrant, the next preferred position p3 the upper left  
810 quadrant and the least preferred position p4 the lower left quadrant. The MUA signal recorded  
811 on channel 14 of this same probe, could have as best preferred position p1 the lower right

812 quadrant, the next best preferred position p2 the upper right quadrant, the next preferred  
813 position p3 the lower left quadrant and the least preferred position p4 the upper left quadrant.  
814 Positions with no significant modulation in any task epoch were labeled as p0 (no selectivity  
815 for this position). Once this was done, for each electrode, pairs of MUA recordings were  
816 classified along two possible functional categories: pairs with the same spatial selectivity  
817 (SSS pairs, sharing the same p1) and pairs with different spatial selectivities (DSS pairs, such  
818 that the p1 of one MUA is a p0 for the other MUA). For the sake of clarity, we do not  
819 consider partial spatial selectivity pairs (such that the p1 of one MUA is a non-preferred, p2,  
820 p3 or p4 for the other MUA).

821 ***MUA layer attribution.*** As stated above, our recordings are not tangential to cortical  
822 surface. As a proxy to attribute a given recording channel to upper or lower cortical layers we  
823 proceeded as follows. For each electrode and each channel, we estimated, at the time of cue  
824 onset in the memory-guided saccade task (100ms-500ms from cue onset), the spike-field  
825 coherence in the alpha range (6 to 16 Hz) and the gamma range (40 to 60 Hz). Based on  
826 previous literature<sup>84</sup>, we used the ratio between the alpha and gamma spike field-coherence as  
827 a proxy to assign the considered LFP signals to a deep cortical layer site (high alpha / gamma  
828 spike-field coherence ratio) or to a superficial cortical layer site (low alpha / gamma spike-  
829 field coherence ratio). We also categorized MUA signals into visual, visuo-motor and motor  
830 categories, as in Cohen et al. (2009). Briefly, average firing rates were computed in 3 epochs:  
831 [-100 0] ms before cue onset (baseline), [0 200] ms after cue onset (visual), and [0 200] ms  
832 before saccade onset (movement). Neurons with activity statistically significantly different  
833 from the baseline (Wilcoxon rank-sum test,  $P < 0.05$ ) after cue onset were categorized as  
834 visual. Neurons with activity statistically significantly different from the baseline (Wilcoxon  
835 rank-sum test,  $P < 0.05$ ) before saccade onset were categorized as oculomotor. Neurons that  
836 were active in both epochs were categorized as visuo-movement neurons. The LFP  
837 categorization along the alpha to gamma spike-field coherence ratio strongly coincided with  
838 the classification of the MUA signals into purely visual sites (low alpha and gamma spike-  
839 field coherence ratio, input FEF layers) and visuo-motor sites (high alpha and gamma spike-  
840 field coherence ratio, output FEF layers, figure 4).

841 ***Noise Correlations.*** The aim of the present work is to quantify task effects onto the  
842 spiking statistics of the FEF spiking activity during equivalent task-fixation epochs. The  
843 statistics that we discuss is that of noise correlations between the MUA activities on the  
844 different simultaneously recorded signals. For each channel, and each task, intervals of

845 interest of 200ms were defined during the fixation epoch from 300 ms to 500 ms from eye  
846 fixation onset. Specifically, for each channel  $i$ , and each trial  $k$ , the average neuronal response  
847  $r_i(k)$  for this time interval was calculated and z-score normalized into  $z_i(k)$ , where  $z_i(k) = (r_i(k) - \mu_i) / \text{std}_i$   
848 and  $\mu_i$  and  $\text{std}_i$  respectively correspond to the mean firing rate and standard deviation  
849 around this mean during the interval of interest of the channel of interest  $i$ . This z-score  
850 normalization allows to capture the changes in neuronal response variability independently of  
851 changes in mean firing rates. Noise correlations between pairs of MUA signals during the  
852 interval of interest were then defined as the Pearson correlation coefficient between the z-  
853 scored individual trial neuronal responses of each MUA signal over all trials. Only positive  
854 significant noise correlations are considered, unless stated otherwise. In any given recording  
855 session, noise correlations were calculated between MUA signals recorded from the same  
856 electrode, thus specifically targeting intra-cortical correlations. This procedure was applied  
857 independently for each task. Depending on the question being asked, noise correlations were  
858 either computed on activities aligned on fixation onset, or on activities aligned on target  
859 (Fixation and Target detection task) or saccade execution (memory guided saccade task)  
860 signals.

861 In order to control for the fact that the observed changes in noise correlations cannot  
862 be attributed to changes in other firing rate metrics, several statistics were also extracted, from  
863 comparable task epochs, from 300 to 500ms following trial initiation and fixation onset. None  
864 of these metrics were significantly affected by the task. Specifically, we analyzed (a) mean  
865 firing rate (ANOVA,  $p > 0.5$ ), (b) the standard error around this mean firing rate (ANOVA,  
866  $p > 0.6$ ), and (c) the corresponding Fano factor (ANOVA,  $p > 0.7$ ). These data, reproducing  
867 previous reports<sup>51,85</sup> are not shown.

868 ***Oscillations in noise correlations.*** To measure oscillatory patterns in the noise  
869 correlation time-series data, we computed, for each task, and each session ( $N=12$ ), noise  
870 correlations over time (over successive 200ms intervals, sliding by 10ms, running from  
871 300ms to 1500ms following eye fixation onset for Fixation and Target detection tasks and  
872 from 300ms to 1500ms following cue offset from Memory-guided saccade task). A wavelet  
873 transform<sup>82</sup> was then applied on each session's noise correlation time series. Statistical  
874 differences in the noise correlation power frequency spectra were assessed using a non-  
875 parametric Friedman test. When computing the noise correlations in time, we equalized the  
876 number of trials for all tasks and all conditions so as to prevent any bias that could be  
877 introduced by unequal numbers of trials. To control that oscillations in noise correlations in

878 time cannot be attributed to changes in spiking activity, a wavelet analysis was also run onto  
879 MUA time series data (data not shown).

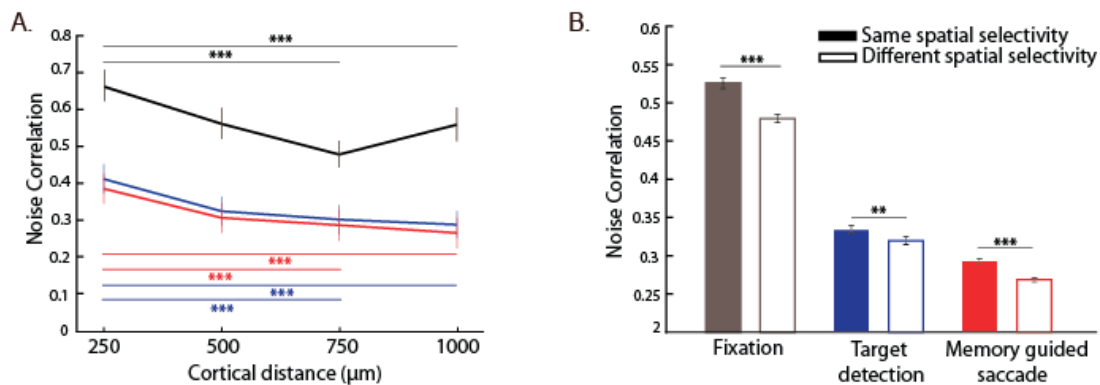
880 ***Modulation of behavioral performance by phase of noise correlation alpha and beta***  
881 ***rhythmicity.*** To quantify the effect of noise correlation oscillations onto behavioral  
882 performance, we used a complex wavelet transform analysis (Fieldtrip, Oostenveld et al.  
883 2011) to compute, for each session and each task, in the noise correlations, the phase of the  
884 frequencies of interest (alpha / beta) following eye fixation onset (for the Fixation and Target  
885 detection tasks) or cue offset (for the Memory guided saccade task). For each session, we  
886 identified hit and miss trials falling at zero phase of the frequency of interest ( $\pm \pi / 140$ ) with  
887 respect to target presentation or fixation point offset time. In the fixation task, premature  
888 fixation aborts by anticipatory manual response or eye fixation failure were considered as  
889 misses. Hit rates (HR) were computed for this zero phase bin. We then shifted this phase  
890 window by  $\pi / 70$  steps and recalculated the HR, repeating this procedure to generate phase-  
891 detection HR functions, across all phases, for each frequency of interest<sup>86</sup>. For each session,  
892 the phase bin for which hit rate was maximal was considered as the optimal phase. The effect  
893 of a given frequency (alpha or beta) onto behavior corresponds to the difference between HR  
894 at this optimal phase and HR at the anti-optimal phase (optimal phase +  $\pi$ ). To test for  
895 statistical significance, observed hit/miss phases were randomized across trials so as to shuffle  
896 the temporal relationship between phases and behavioral performance. This procedure was  
897 repeated 1000 times. 95% CI was then computed and compared to the observed behavioral  
898 data.

899 ***Spikes-LFP Phase coupling.*** For each selected channel, spikes-LFP phase coupling  
900 spectra (SFC) were calculated between the spiking activity obtained in one channel and the  
901 LFP activity from the next adjacent channel in the time interval running from 300ms to  
902 1500ms following cue offset. We used a single Hanning taper and applied convolution  
903 transform to the Hanning-tapered trials. We equalized the number of trials for all conditions  
904 so as to prevent any bias that could be introduced by unequal numbers of trials. We used a 4  
905 cycles length per frequency. The memory guided saccade task is known to involve spatial  
906 processes during the cue to target interval that bias spike field coherence. Thus, spikes-LFP  
907 phase coupling was measured separately for trials in which the cued location matched the  
908 preferred spatial location of the channel and trials in which the cued location did not match  
909 the preferred spatial location of the channel. Statistics were computed across channels x  
910 sessions, using a non-parametric Friedman test.

911

912 **Supplementary figures**

913



914

915 **Figure S1: (A) Noise correlations as a function of cortical distance.** Average noise  
916 correlations (mean +/- s.e.) across sessions, for each task (conventions as in (A)), from 300  
917 ms to 500ms after eye fixation onset, as a function of distance between pairs of channels:  
918 250μm; 500μm; 750μm; 1000μm. Stars indicate statistical significance following a two-way  
919 ANOVA and ranksum post-hoc tests; \*p<0.05; \*\*p<0.01; \*\*\*p<0.001. (B) **Noise**  
920 **correlations as a function of spatial selectivity.** Average noise correlations (mean +/- s.e.)  
921 across sessions, for each tasks (conventions as in figure 2), from 300ms to 500ms after eye  
922 fixation onset, as a function of whether noise correlations are calculated over signals sharing  
923 the same spatial selectivity (full bars) or not (empty bars). Stars indicate statistical significance  
924 following a two-way ANOVA and ranksum post-hoc tests; \*p<0.05; \*\*p<0.01; \*\*\*p<0.001.

925

926

927

928

929

930

931